RADIATION TESTING OF OPTICAL FIBERS AND PHOTOTRANSISTORS

Fouad A. S. Soliman*

Nuclear Materials Authority
Maadi P.O.Box 530, Cairo
Egypt

and

Hoda A. Ashry

National Center for Radiation Research and Technology
Egypt

الخلاصـة :

يشتمل البحث على دراسة مستفيضة عن سلوك أنظمة الاتصالات ونقل المعلومات باستخدام شبكة الألياف الضوئية ومكوناتها المختلفة وذلك عند الطول الموجي للضوء عند التشغيل (٨٥٠ ، ١٣٠٠ نانوميتر) . وقد وجُد أن حساسية التغير في خواصها الطبيعية والكهربائية عند التعرض للإشعاع الجامي عالية مؤدية الى زيادة كبيرة في نسبة الفقد في نقل طاقة الضوء وكثافته وتشتته ، ووجُد أن نسبة الفقد هذه تمثل دالة خطية في الجرعة الاشعاعية الساقطة بدءاً من مستوى أشعاع في حدود (٢٠٠٠) راد .

عند اختبار الخواص الكهربائية لكاشف المستوى الضوئى (الموحد الضوئى) النافذ من شبكة الألياف وذلك تحت تأثير الاشعاع وجد أن هذا التعرض يؤدي الى توالد تيار قصر وقتي تتناسب شدته مع معدل جرعة التشعيع وذلك حتى مستوى ٣٨٠ راد/ثانية . وعند زيادة الجرعة الاشعاعية الممتصة بالكاشف فإن حساسية استجابته للضوء الساقط وكفاءة تحويل الطاقة الضوئية الى طاقة كهربائية تقل بشدة ، وان قيمة كفاءة تحويل ابتدائية قدرها ٧٣٪ تنخفض الى ٥٤٪ ، ١٨٪ نتيجة التعرض لجرعة اشعاعية قدرها ٧٠ ، ١٤٠ ميجا راد على التتابع .

امتدت الدراسة كذلك الى الكاشف الضوئى الثلاثى الوصلة (ترانزستور ضوئى) والذي يتمتع بكفاءة كشف ضوئى فائقة ، وقد تسبب التعرض الاشعاعي في هبوط معامل تكبير الكاشف من ١٢٠٠ إلى ٩٠٠ ، ٤٠٠ عند مستوى جرعات ٩٠ كيلوراد ، ١١٤٠٠ كيلوراد .

تبيَّـن من الدراسة مدى الحساسية العالية لانظمة الاتصالات المقترحة لاشعة جاما ، كما ثبت بنجاح إمكانية تطبيق استخدام تلك المكونات كمقياس للجرعات الاشعاعية التي يمكن ان تتعرض لها والتي يمكن منها تقدير أعمار الحياة لتلك الانظمة عند تطبيق استخدامها في نقل المعلومات في مجالات قد تؤدى إلى تعرضها للإشعاع النووي .

* To whom correspondence should be addressed.

ABSTRACT

Tests have been performed to examine the effects of γ-exposure on opto-electronic components that can be used in digital fiber optic data links. The response of fiber wave guides to ionizing radiation has been studied. Measurements of the growth and decay of the radiation induced loss at 850 nm and 1300 nm have revealed that fibers are sensitive to γ-dose. In addition, a linear dependence of short circuit current on γ-dose rate, up to 380 rad/sec, for the photodiode was shown. At very high dose levels, permanent damage is noticed in the diode characteristics and its current decreases, where a value of 1600 μA, measured at light intensity level of 8000.0 lux, dropped to 1200, 950, 820, 700, 600, and 550 μA after γ-exposure up to 2.0, 16, 38, 70, 105, and 140 Mrad respectively. Also, the forward current gain factor of phototransistors, measured as a function of operating collector current, shows a severe decrease due to γ-exposure. The damage effect has minima that usually corresponds to the lower and higher ends of the operating collector current range of a device. Finally, proposals using photodiodes for gamma dose- and dose rate-dosimetry are given, tested, and proved to be quite satisfactory.

RADIATION TESTING OF OPTICAL FIBERS AND PHOTOTRANSISTORS

INTRODUCTION

For many years we have been using radio waves or copper wire to carry messages around the world. The radio waves are filling up rapidly and hence, this resource is beginning to run out. Similarly, copper wire is only able to carry information at a limited speed, although the use of coaxial cable does allow some improvement to be made in this respect. Unfortunately coaxial cable is very bulky, very expensive and only likely to increase in price as reserves of copper run out. Finally, the bandwidth available on coaxial cables is inversely proportional to the square of the length of cable. The use of fiber optic cables where bandwidth is inversely proportional to length, increases the band width available for long distance communications, providing an expandable medium to meet the increasing demands for information to be sent worldwide. They are now being considered for use in many military and industrial applications. In general, fiber optic wave guides are light weight, provide large bandwidth for multiplexing, and are expected to result in a substantial reduction in system cost [1–4].

1.1. Fibers

Optical fiber is made of two parts, the core and the cladding (Figure 1). When we try to inject light into an optical fiber, it needs to strike the core/cladding boundary at less than the critical angle of that boundary, to permit reflection along the core. If the angle is great, the beam will be refracted into the cladding and lost. Therefore a very small light source is needed, accurately aligned with the fiber core to transmit all the available power into the cable.

1.1.1. Fiber Basic Types

1.1.1.1. Multi Mode Step Index. For fiber with a very large diameter (200 μm; Figure 2), light travels in every direction at once. This characteristic enables the light to propagate along fiber using thousands of different paths, modes. In a straight length of cable, one light mode will be exactly parallel to the direction of the cable. This, therefore is the shortest path and the light traveling along this path will arrive first. The remaining light will arrive

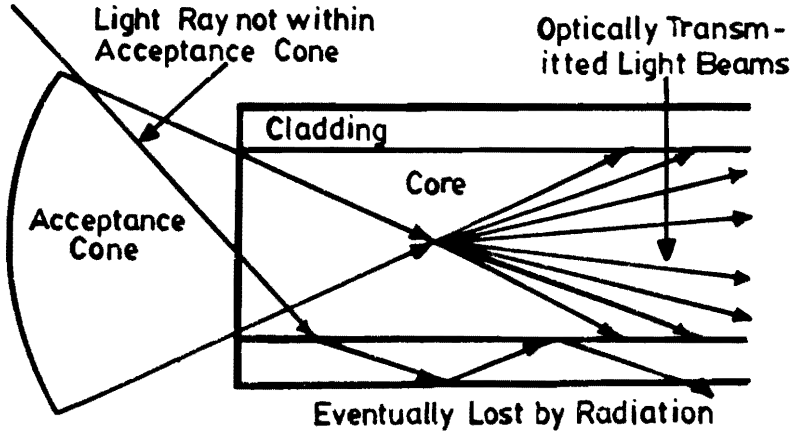

Figure 1. Light Modes Through Fiber.

later, the length of delay increasing with the number of reflections encountered. Light injected "at the same time" into one end of the fiber arrives at the other end spread out over a period of time. This is called modal or multi mode dispersion. If the input pulse is heavily dispersed, it can greatly reduce the amplitude of the signal (attenuation) since the total energy of the signal remains constant.

1.1.1.2. Multi Mode Graded Index. In case of fibers with a much smaller core of a graded index construction, light bends progressively down the core reducing the number of propagation modes allowed and hence the broadening effects.

1.1.1.3. Single Mode Step Index. Finally, for the very fine core cable (<10 μm), the light propagates along a single path only, this removes the pulse spreading associated with multiple modes.

1.1.2. Optical Power Losses

Signal attenuation in optical fibers originates from four main mechanisms: absorption, scattering, wave guide imperfections, and interconnections.

1.1.2.1. Absorption. The intrinsic absorption loss of high silica glasses in the near infrared region of the spectrum is composed of (Figure 3). (*a*) *Ultraviolet absorption,* which results from the electronic bands of the constituent materials; and (*b*) *Infrared absorption,* which results from very strong cation–oxygen vibrational modes of the glass lattice. On the other hand, extrinsic sources of absorption include hydroxyl ions (OH^{-1}) and transition metal ions. The latter, at the level of a few ppb's, can cause unacceptably high absorption losses.

1.1.2.2. Scattering. Rayleigh scattering results from compositional and density fluctuation over distances much smaller than the wavelength of light. The Rayleigh scattering together with the IR and UV absorption define an intrinsic transmission window extending from 0.70 to 1.80 μm, with the minimum loss occurring in the 1.55 μm region for fibers lightly doped with GeO_2. This intrinsic window together with the OH absorption bands at 1.390 μm, 1.250 μm, and 0.95 μm define three operating bands centered around 0.85 μm, 1.30 μm, and 1.55 μm respectively.

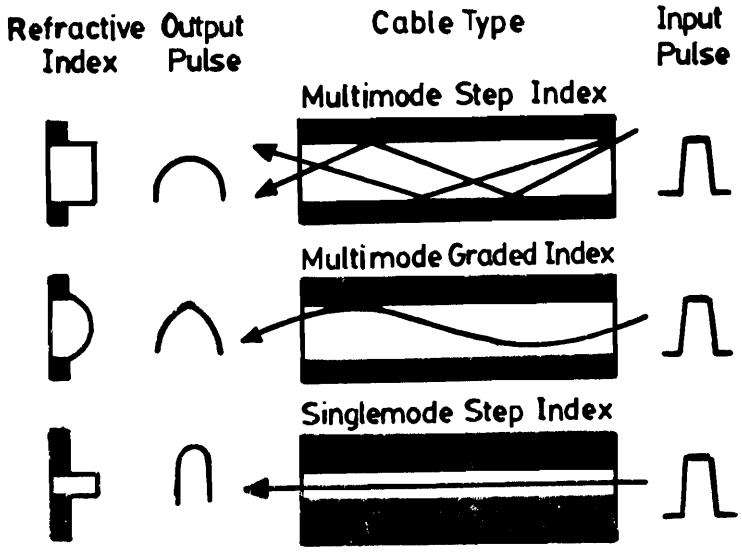

Figure 2. The Three Basic Fiber Types.

1.1.2.3. Wave Guide Imperfections (Figure 4). These imperfections are mainly geometrical effects such as: (*a*) *Irregularities* like core geometry variations and core cladding interface imperfections; (*b*) *Micro bends* (microscopic random bends) resulting from coating and cabling; and (*c*) *Curvature or bends* in the installed cable specially at the distributing frames at the terminals.

1.1.2.4. Interconnection Loss. These are losses arising when two fibers are either connected or spliced together. The losses are due to alignment problems and geometry and refractive index differences between fibers.

1.2. Photodiode

A photodiode has a depleted semiconductor region with a high electric field that serves to separate photo generated electron hole pairs. For high-speed operation, the depletion region must be thin to reduce the transit time.

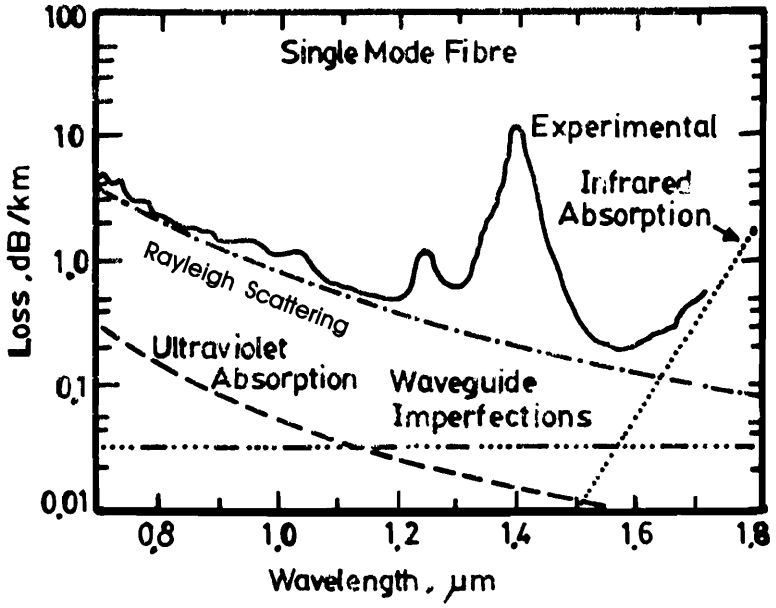

Figure 3. Observed Loss Spectrum of a Germanosilicate Single-Mode Fiber.

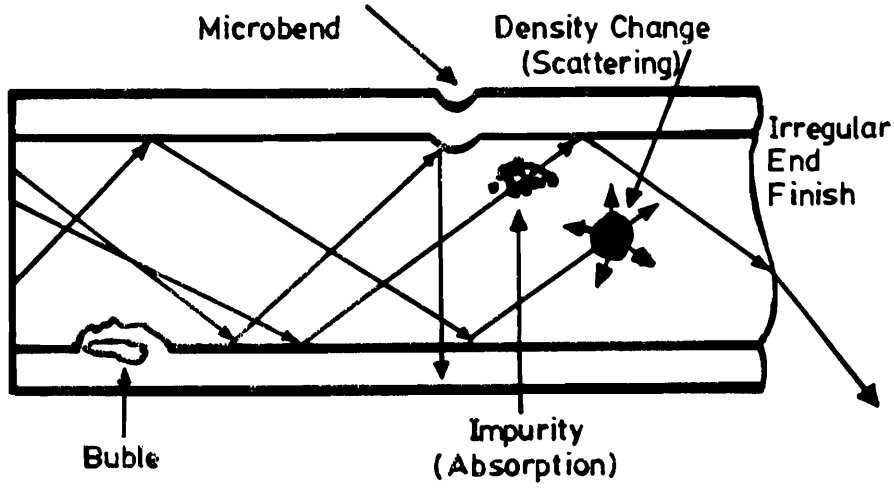

Figure 4. Optical Power Loss Sources.

On the other hand, to increase the quantum efficiency, the depletion layer must be sufficiently thick to allow a large fraction of the incident light to be absorbed. Thus there is a trade-off between the speed of response and quantum efficiency [5, 6]. For a photodiode only a narrow wavelength range centered at the optical signal wavelength is important. For the visible and near-infrared range, photodiodes are usually reverse biased with relatively large biasing voltages, because this reduces the carrier transit time and lowers the diode capacitance. The biasing condition is in contrast to avalanche photodiodes, where an internal current gain is obtained as a result of the impact ionization under avalanche breakdown conditions.

1.3. Phototransistor

The phototransistor is a much more sensitive semiconductor photodevice than the photodiode [7, 8]. It is usually connected in a common-emitter configuration with the base open, and radiation is concentrated on the region near the collector junction (Figure 5). The operation of this device can be understood if we recognize that the emitter junction is slightly forward biased. Assuming, first, that there is no radiant excitation, minority carriers are generated thermally, and the electrons crossing from the base to the collector, as well as the holes crossing from the collector to the base, constitute the reverse saturation collector, I_{co}. The collector current is given by:

$$I_c = (1 + \beta)\ I_{co} + \beta I_B, \tag{1}$$

where, I_B is the base current, then, at $I_B = 0$, one gets;

$$I_c = (\beta + 1)\ I_{co}. \tag{2}$$

If the light is now turned *ON*, additional minority carriers are photo-generated, and these contribute to the reverse saturation current in exactly the same manner as do the thermally-generated minority charges. If the component of the reverse saturation current due to the light is designated I_L, the total collector current is:

$$I_c = (\beta + 1)\ \ (I_{co} + I_L). \tag{3}$$

We note that, due to transistor action, the current caused by radiation is multiplied by the large factor $(\beta + 1)$.

1.4. Radiation Effects

When high energy radiation falls on a semiconductor device, energy is deposited in the semiconductor *via* two mechanisms: atomic displacement and ionization. The relative importance of these two mechanisms in a

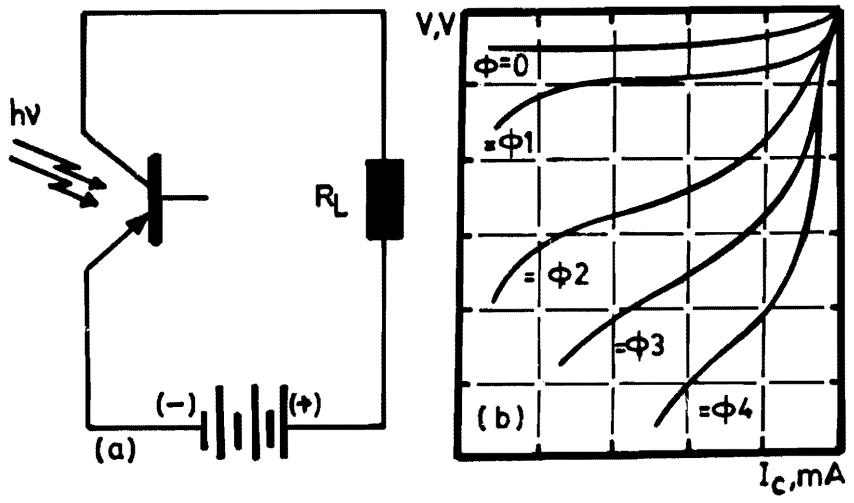

Figure 5. Connection Diagram (a) *and a Set of Collector Current–Voltage Curves* (b) *for a Phototransistor Under Different Illumination Levels.* ($\phi 4 > \phi 3 > \phi 2 > \phi 1$)

semiconductor depends on both the type of radiation and the nature of the device. The initially-produced defect for γ- and electron-irradiation is quite simple and can be expressed as a single displaced atom and its associated vacancy. The interaction is simply described by the number of defects/cm^3 created, which is given by [9, 10]:

$$N_f = \phi \cdot \sigma_d \cdot N_o. \tag{4}$$

where:

ϕ : radiation fluence
σ_d : displacement cross-section/cm^2
N_o : number of lattice atoms/cm^3.

2. EXPERIMENTAL PROCEDURE

Three γ-cells were used in the present investigation [9]. The first was a "GC-220" having a Co-60 source with dose rate of 8.0 rad/s. The second was "GC 4000A" having a Co-60 source of a dose rate of 130 rad/s and the third one was the "J-6500" irradiator which furnished with a Co-60 source plaque and used for high radiation levels where dose rate distribution was measured, calculated, and reported [11].

Several of the investigated devices (fiber links, photodiode type "TESLA 1PP75P+" and phototransistor type GEL 1463) were exposed to γ-ray in steps up to a total dose of 15.0 krad for fibers and 140 Mrad for photodevices. The photodevice reverse dark current dependence on γ-dose rate was measured using the first and second γ-cells. For higher dose levels, samples were fixed at different distances opposite to the source plaque of the third irradiator while recording the change or in the photocurrent. The experimental work has been extended to include the permanent damage which may occur due to high γ-exposure levels up to 140 Mrad.

3. RESULTS AND DISCUSSIONS

3.1. Radiation Effects on Fiber Links

A pulse of radiation impinging on the fiber causes absorption and luminescence [12, 13]. The luminescence is a maximum during the radiation pulse and negligible thereafter. Immediately following irradiation, the induced absorption is a maximum and decays with time to some permanent value. These effects result from the irradiation of optical materials by γ-rays, electrons, or X-rays. The incident photons produce energetic electrons in the glass network which dissipates energy by the formation of electron–hole pairs or free radicals. While most of these pairs undergo recombination, a small fraction of both holes and electrons become trapped at imperfections in the lattice. Some of these trapped charges or free radicals result in optical absorption. In addition, luminescence may be emitted during irradiation, and de-excitation processes. Alternatively, the irradiation energy may be imparted to the lattice in the form of heat as in the production of defects. Those defects, particularly when populated with charges may also be observed as absorption. Virtually all fibers of this type are extremely sensitive to ionization radiation. For example, the radiation induced optical loss *versus* γ-ray dose, measured at 850 nm and 1300 nm, is shown in Figure 6. Below 2000 rad, the fiber illustrates much greater losses per unit dose. Above this dose levels, the change in the induced loss is shown to be insignificant. One of the conclusions of this study is that there is no dose-rate dependence of the radiation induced attenuation. Another finding of these studies was that the radiation induced attenuation tended to saturate [14].

The analytical model for the attenuation (A) must take into account the generation rate and recovery rate (R) of the attenuation [15]. The recovery in fiber is easy to determine. It has been found to depend on $t^{-1/4}$, where "t" is the time since production. The generation is harder to determine exactly, however, it was found that, for short exposure, the production was sub-linear with dose and could be reasonably described by:

$$A(t) = A_o \phi^x. \tag{5}$$

where, x is between 3/4 and 4/5.

This is almost certainly a dose dependence since it has been found that the attenuation produced is independent of dose rate when recovery is allowed, and the generation-rate is:

$$G(t) = G_0 . \phi^{x-1} . d\phi/dt. \tag{6}$$

Substituting the product of the dose-rate ϕ and time (t) for "ϕ" gives:

$$G(t) = G_0(\dot{\phi})^x . (t)^{x-1} \tag{7}$$

The recovery equation is:

$$R(t) = R_0 . t^{1/4}. \tag{8}$$

Assuming $X=3/4$, fiber length = 4 m, and fitting the pulsed data gives the following constants: $G_0=0.8$ and $R_0=2\times10^{-4}$. This effectively assumes that the annealing begins at 100 nsec, and for constant flux, the attenuation at time "t" is:

$$A(t) = 4.5\times10^{-3}\ \phi^{3/4}\ t^{1/2}. \tag{9}$$

Following exposure, the transmission of a fiber data link increase toward the pre-irradiated value (Figure 7), where room temperature recovery curve follows a power law, and the attenuation never recovers beyond the originally present value.

3.2. Effects on Photodiodes

Photodiodes, which are a key element in optical subsystems have one drawback from a radiation point of view; they have a relatively large active volume compared with other semiconductor devices. The large volume results in a high sensitivity to ionization-induced transients. Compounding this problem in optical subsystems is the fact that receivers are often operated in a very high gain condition to provide the sensitivity that many of the optical subsystems require. These two features combine to produce ionization induced transient photocurrents which cause an upset in optical subsystems at relatively low radiation levels.

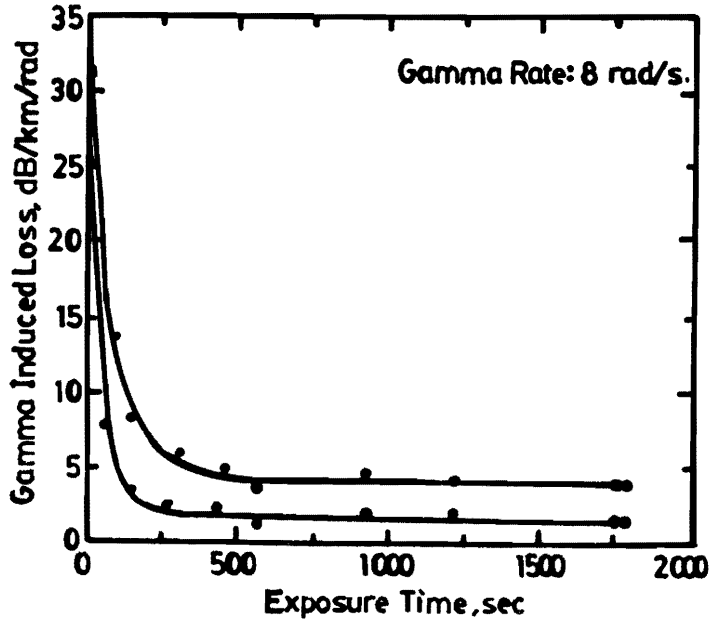

Figure 6. Gamma-Induced Optical Loss versus *Exposure Time.*

3.2.1. Collection Efficiency

Representative results for the investigated photodiode, in the light wavelength band from 500 nm to 800 nm, under the influence of γ-radiation were shown. Figure 8 represents the spectrum for the cells, from which it is clear that most sensitive wavelengths are concentrated within the band from 540 nm up to around 750 nm. Also, the same Figure shows the effect of γ-radiation, where it is found that the device collection efficiency value was decreased from 73% down to a certain values of 54% and 18% due to γ-exposure up to 70 and 140 Mrad respectively.

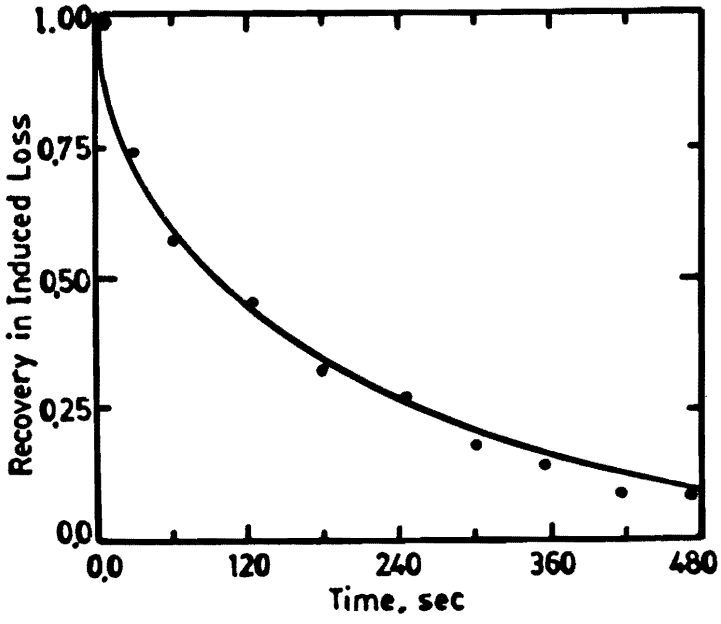

Figure 7. Recovery of Radiation-Induced Absorption After Exposure to Gamma Doses up to 15 krad.

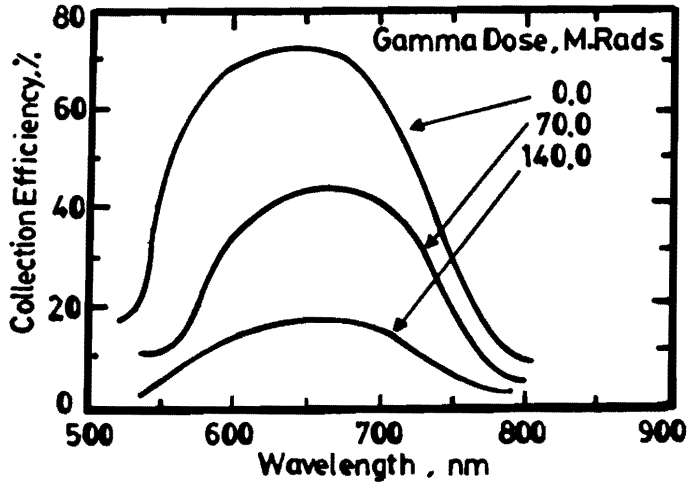

Figure 8. Representative Collection Efficiency Data for Photodiode.

3.2.2. Volt–Ampere Characteristics

The electrical properties of the photodiode show a strong dependent on light illumination intensity and γ-exposure. Figure 9 represents the changes in the $(I-V)$ characteristics of the devices under the influence of light exposure up to 23.5 klux (solid lines) and the same curves after γ-exposure up to 70 Mrad (dashed lines). The dark current (I_o) corresponds to the reverse saturation current due to thermally generated minority carriers, these minority carriers "fall down" the potential hill at the junction. Now if light falls upon the surface, additional electron–hole pairs are formed. These injected minority carriers diffuse to the junction, cross it, and contribute to the current (I_s). Hence, the $(I-V)$ characteristics is given by:

$$I = I_s + I_o(\exp(-V/\beta V_T). \tag{10}$$

where, V_T is the volt equipment of temperature, and β is a constant which equals 1 for Ge and 2 for Si.

3.2.3. Transient Effects

Figure 10 illustrates the rise- and fall-times of the reverse dark current (photocurrent) for the photodiode under the influence of γ-radiation with dose-rate of 138 rad/s. The data obtained show that the time required for the photocurrent to reach its steady state value is something around 4 – 5 seconds, which agrees approximately with the reading time of the digital electrometer (Keithley 616). But it has been reported that the time required for the charge carrier to reach its steady state value is in the μsec range [11]. Hence, both of times are dependent on a certain time constant which controls the process (RC of the measuring circuit), and are independent of the amplitude of the current.

3.2.4. Dose Rate Dependence

The γ-radiation induced dark current in the photodiode is shown in Figure 11. A linear dependence of reverse current on the dose rate is obtained within a γ-dose rate range up to 390 rad/s. The obtained results are found to

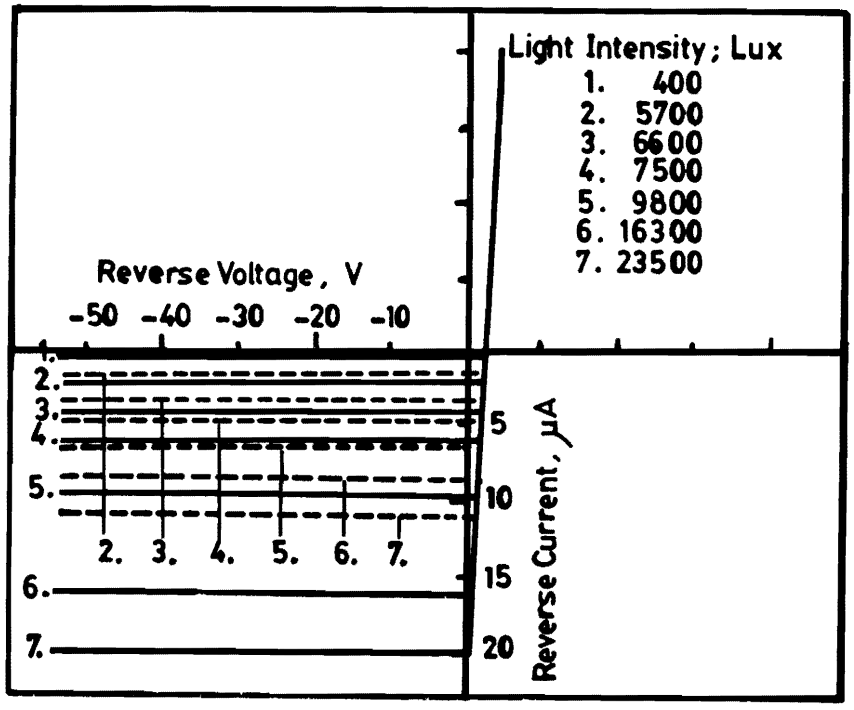

Figure 9. (I–V) Characteristics of the Photodiode. Dashed Lines are for Samples Irradiated up to 70 Mrad.

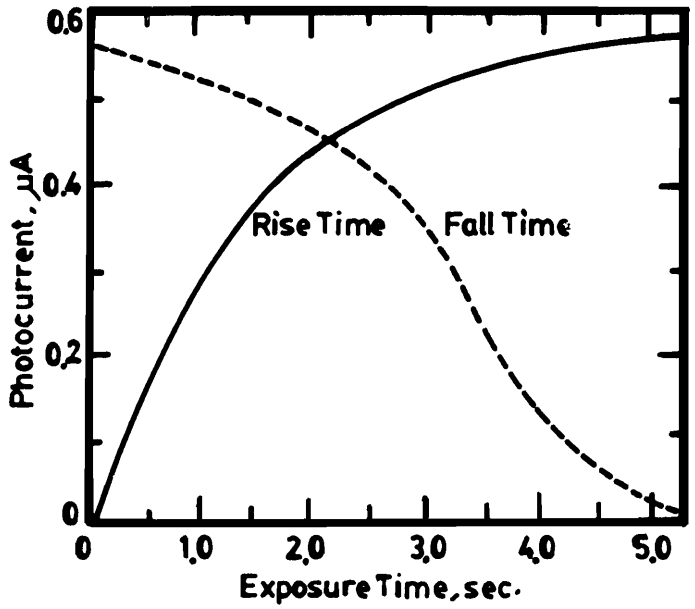

Figure 10. Rise- and Fall-Time of Photocurrent in the Photodiode due to 138 rad/sec Gamma Dose.

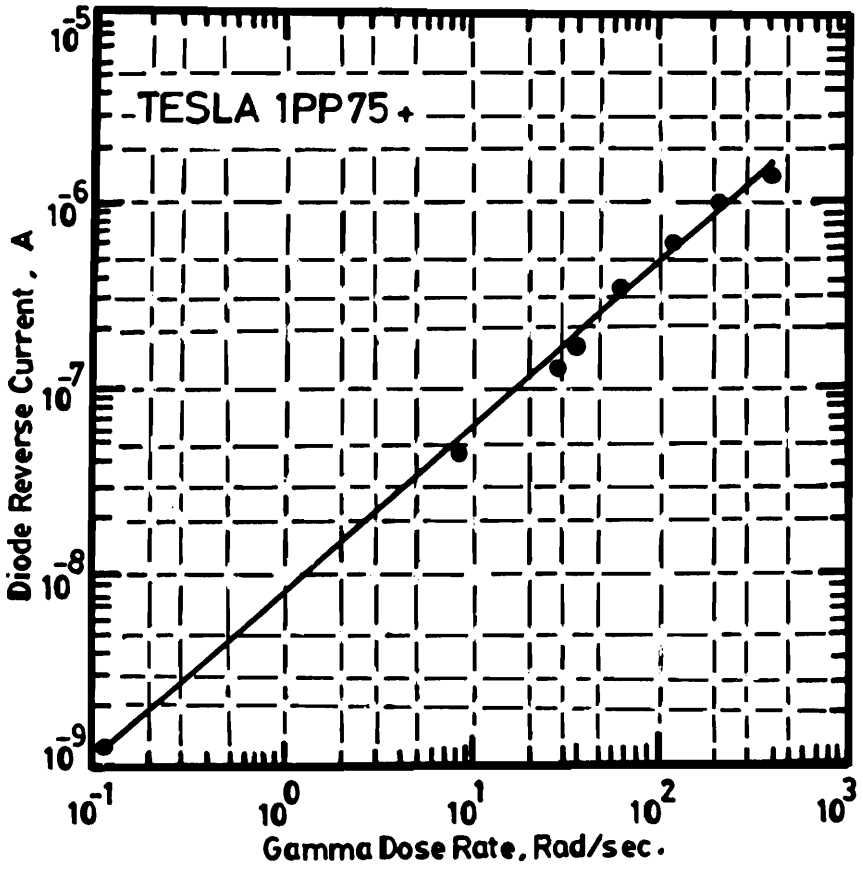

Figure 11. Dose Rate Dependence of the Photodiode Reverse Current.

confirm those experimental and theoretical results published previously [11]. The high sensitivity of such devices is again in reasonable agreement with the known device area. These results lead to the possibility of the application of photodiodes as a dose rate meters, at least within the available dose range (8.0 rad/s up to 390 rad/s). From Figure 11, a proportionality constant can be deduced for the sensitivity of the investigated photodiode type (18 μA/rad/s).

At very high dose levels, permanent damage is noticed in the diode characteristics and the current is shown to decrease; a value of 1600 μA, measured at a light intensity level of 8000 lux, was dropped to 1200, 950, 820, 700, 600, and 500 μA after γ-exposure up to 2.0, 16, 38, 70, 105, and 140 Mrad respectively (Figure 12).

3.3. Effects on Phototransistors

Figure 13 represents a typical DC-output characteristics for a phototransistor before and after γ-exposure. Continuous lines represent the initial DC-output characteristics at different light illumination levels; while dashed and dotted lines represent the same characteristics after exposing the device to γ-exposure up to 90 krad and 11.40 Mrad respectively. Higher absorbed doses were found to produce insignificant changes.

Detailed study was performed on the investigated transistors type and their forward current gain factors (h_{FE}) were plotted. The radiation damage effects as a function of the operating current during measurement of the forward current gain changes is shown in Figure 14. It is clear that at operating collector current values less than 0.1 mA and higher values than 300 mA the damage effect has a minimum that usually corresponds to the low and high ends of the operating range of a device. Maximum damage effects appear to be at collector current value around 8–10 mA where the forward current gain values of 900 and 750 were shown although its initial value is 1200 (Figure 15).

The degradation of transistor parameters is due to both structural damage in the crystal lattice and to changes in the surface properties of the crystals [16]. A change in the recombination properties of surface layer, particularly in the immediate vicinity of the emitter p–n junction affects the base current transport coefficient. The production of

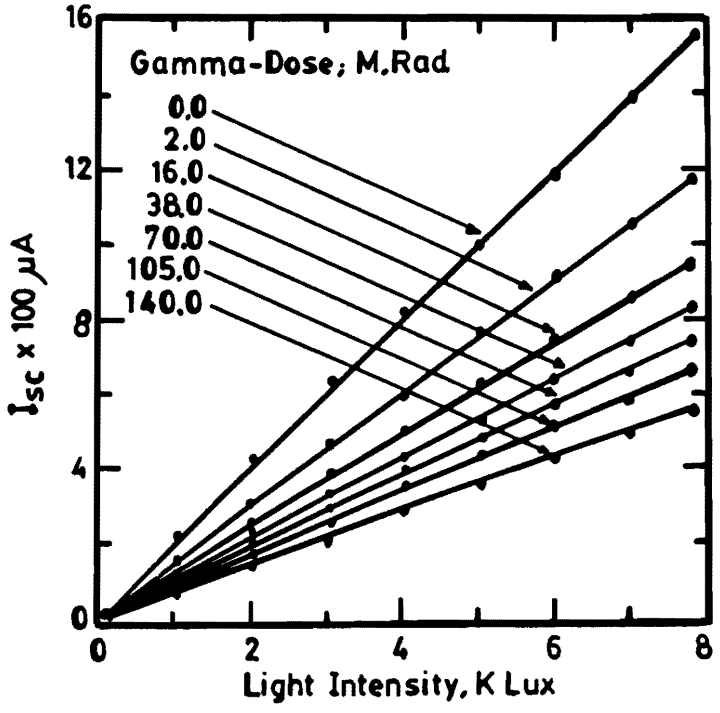

Figure 12. Gamma Radiation Effects on (I_{sc}/Light Intensity) Relationship for Photodiodes.

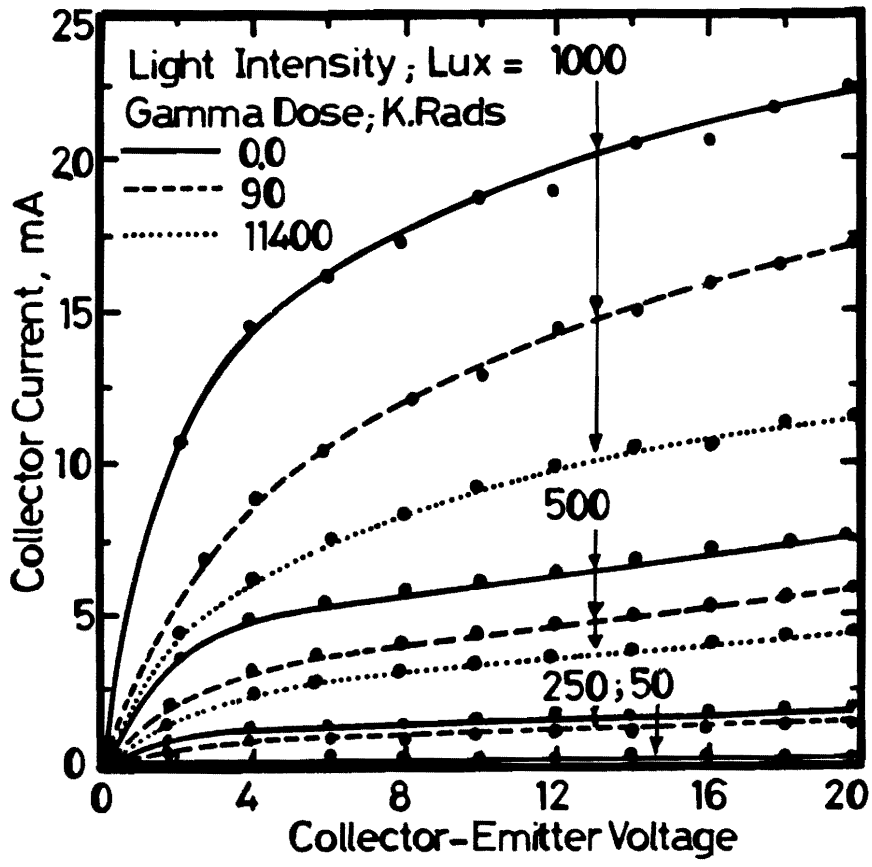

Figure 13. DC-Output Characteristics for a Phototransistor, with Base Floated, Before and After Gamma Exposure.

inversion layers and of surface channels in vicinity of p – n junctions leads to a considerable increase in the reverse currents across the junctions. Surface effects are caused primarily by ionization phenomena in the oxide layers of crystals and in their immediate vicinity. This explains why such effects are so easily induced by high energy radiation as well as by low-energy radiation which cannot cause bulk damage.

4. CONCLUSIONS

The testing reported here examined the effect of γ-exposure of some opto-electronic components. In conclusion, present day commercial fibers may have limited use in radiation hardened systems. The silica fibers are very sensitive to radiation. Besides, the values of the short circuit current of photodiode and forward current gain factor of phototransistors were dropped severely under the influence of γ-exposure.

REFERENCES

[1] J. Senior, *Optical Fiber Communications: Principles and Practice.* London: Prentice–Hall, 1985.

[2] *DOD Integrated Optics and Fiber Optics Communications Conference, San Diego, CA, USA,* May 15–17, 1974.

[3] M. H. Aly, "Characterization of Single-Mode Optical Fibers Far From Field Intensity Pattern", *8th National Radio Conference, Cairo,* February 19–21, 1991, vol. 4, D7, pp. 1–7.

[4] S. F. Mahmoud and A. M. Kharbat, "Analysis and Application of a Coaxial Optical Fiber Line", *8th National Radio Conference, Cairo,* February 19–21, 1991, vol. 4, D6, pp. 1–8.

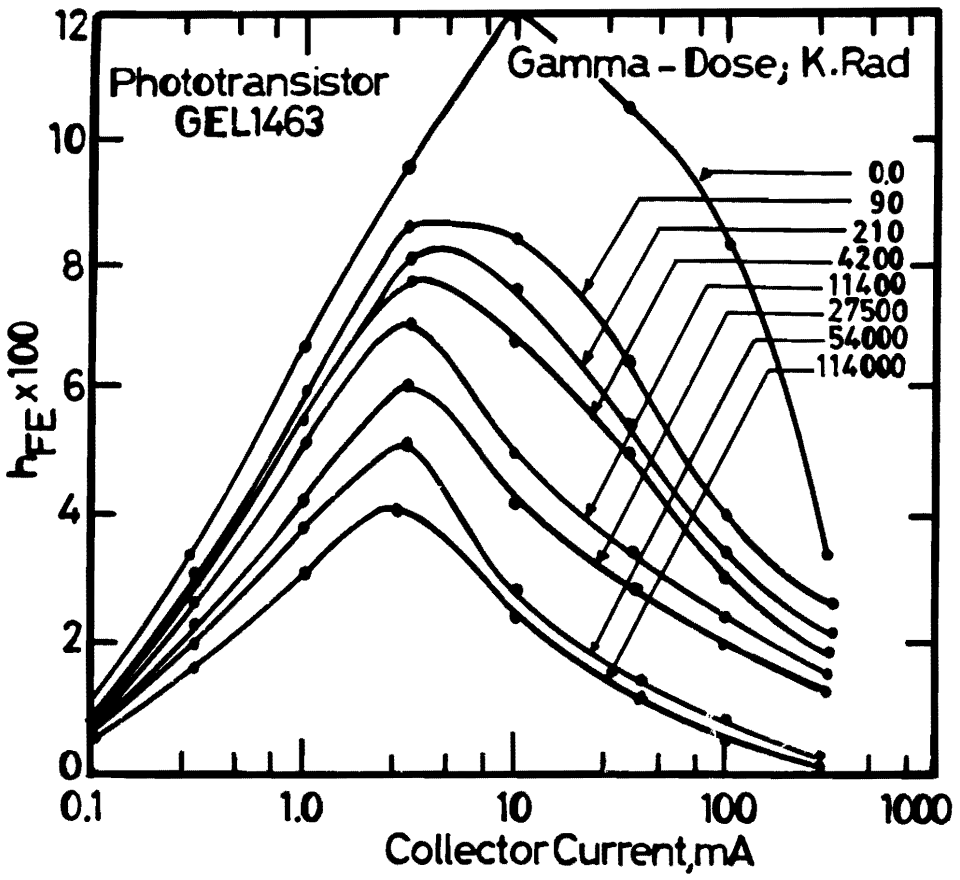

Figure 14. Forward Current Gain Factor as a Function of Collector Current and Gamma Dose.

[5] F. A. S. Soliman, M. H. El-Fouly, M. B. Saleh, and M. El- Ashry, "Fabrication and Characterization of Silicon Photovoltaic Cells for Solar Energy Conversion", *World Renewable Energy Congress, Reading, U.K.*, 23–28 September 1990, Oxford: Pergamon Press (ISBN 008 0375313), vol. 1, pp. 135–140.

[6] F. A. S. Soliman, M. H. El-Fouly, A. A. El-Halim, and M. El-Ashry, "Application of Silicon Photovoltaic Cells in Detection Electromagnetic Waves", *World Renewable Energy Congress, Reading, U.K.*, 23–28 Sep. 1990, Oxford: Pergamon Press (ISBN 008 0375313), vol. 1, pp. 337–342.

[7] V. Stupelman and G. Filaretov, *Semiconductor Devices*. Moscow: Mir Publisher, 1976.

[8] S. M. Sze, *Physics of Semiconductor Devices*. New York: Wiley, 1981.

[9] M. S. Rageh, M. Marzouk, and F. A. S. Soliman, "Gamma-Radiation Effects on the Electrical Properties of Optoelectronic Devices", *Egypt. J. Rad. Sci., Appl.*, **4(1)** (1987), pp. 85–104.

[10] F. A. S. Soliman, M. S. I. Rageh, and A. Z. El-Behay, "Effects of Electron Irradiation on Silicon Photovoltaic Cells", *Isotopenpraxis*, **22(3)** (1991), pp. 147–149.

[11] M. S. I. Rageh, A. Z. El-Behay, and F. A. S. Soliman, "Application of Commercial Silicon Diodes for Dose Rate Measurements", *Int. Symp. of High-Dose Dosimetry, IAEA , SM 272/30, Vienna*, 8–12 October 1984.

[12] E. J. Friebele, "Optical Fiber Waveguides in Radiation Environments", *Optical Eng.*, **18** (1979), pp. 552–561.

[13] C. J. Dale and E. A. Burke, "Space Radiation Effects on Opto-electronic Materials and Components for a 1300 nm Fiber Optic Data Bus", *IEEE Trans. Nucl. Sci.*, **NS-39(6)** (1992), pp. 1982–1989.

[14] P. L. Mattern *et al.*, *IEEE Trans. Nuc. Sci.*, **NS-22** (1975), p. 2468.

[15] B. D. Evans and G. H. Sigel, Jr., *IEEE Trans. Nuc. Sci.*, **NS-21** (1974), p. 113.

[16] F. A. S. Soliman, "Some Analysis of Radiation Effects on PNP Devices", *Isotopenpraxis*, **26(5)** (1991), pp. 225–229.

Paper Received 19 September 1992; Revised 26 January 1994; Accepted 2 April 1994.